Cellular Physiology and Biochemistry

Cell Physiol Biochem 2017;43:1168-1187
DOI: 10.1159/000481758
Published online: October 05, 2017
Accepted: August 10, 2017

Original Paper

Exogenous H_2S Protects Against Diabetic Cardiomyopathy by Activating Autophagy via the AMPK/mTOR Pathway

Fan Yang Linxue Zhang Zhaopeng Gao Xiaojiao Sun Miao Yu Shiyun Dong Jichao Wu Yajun Zhao Changqing Xu Weihua Zhang Fanghao Lu

Department of Pathophysiology, Harbin Medical University, Harbin, China

Key Words
Diabetic Cardiomyopathy • Oxidative Stress • Apoptosis • Autophagy • AMPK/mTOR

Abstract
Background/Aim: Autophagy plays an important role in cellular homeostasis through the disposal and recycling of cellular components. Hydrogen sulphide (H_2S) is the third endogenous gas that has been shown to confer cardiac protective effects. Given the regulation of autophagy in cardioprotection, this study aimed to investigate the protective effects of H_2S via autophagy during high glucose treatment. ***Methods:*** This study investigated the content of H_2S in the plasma as well as myocardial, ultrastructural changes in mitochondria and autophagosomes. This study also investigated the apoptotic rate using Hoechst/PI as well as expression of autophagy-associated proteins and mitochondrial apoptotic proteins in H9C2 cells treated with or without GYY4137. Mitochondria of cardiac tissues were isolated and RCR and ADP/O were also detected. AMPK knockdown was performed with siRNA transfection. ***Results:*** In a STZ-induced diabetic model, NaHS treatment not only increased the expression of p-AMPK in diabetic group but further activated cell autophagy. Following 48h high glucose, autophagosomes and cell viability were reduced. The present results showed that autophagy could be induced by H_2S, which was verified by autophagic ultrastructural observation and LC3-I/LC3-II conversion. In addition, the mitochondrial membrane potential (MMP) was significantly decreased. The expressions levels of autophagic-related proteins were significantly elevated. Moreover, H_2S activated the AMPK/rapamycin (mTOR) signalling pathway. **Conclusions:** Our findings demonstrated that H_2S decreases oxidative stress and protects against mitochondria injury, activates autophagy, and eventually leads to cardiac protection via the AMPK/mTOR pathway.

Introduction

In diabetic patients, a wide range of structural reconfigurations have been observed, such as cardiomyocyte hypertrophy, ventricular dilation, prominent interstitial fibrosis

Professor Weihua Zhang
and Fanghao Lu

Department of Pathophysiology,
Harbin Medical University, Harbin, (China)
Fax +86-451-86674548, E-Mail zhangwh116@126.com, lufanghao1973@126.com

[1, 2], diastolic dysfunction, systolic dysfunction, and left ventricular hypertrophy [3, 4] _ ENREF_4.This disease process is known as diabetic cardiomyopathy (DC), which is a cardiac muscle-specific disease without other vascular pathology_ENREF_6.

Macroautophagy (henceforth, 'autophagy') at a low level under physiological conditions exerts its cellular protective and quality control process, which can be activated in response to stress conditions including starvation and oxidative stress [5]. Autophagy is an evolutionarily conserved catabolic process to degrade and recycle long-lived proteins and damaged organelles [6]. The mechanisms of the autophagy induction are not entirely clear. Much of the research has established the role of autophagy in the development of diabetic cardiomyopathy [7]. It has been reported that both apoptosis and autophagy are essential for cell survival [8]. Well-established type 1 diabetic animal models, namely STZ-induced diabetic mice [9] and OVE26 mice [10], exhibit inhibited of cardiac autophagy along with cardiomyocyte apoptosis and cardiac dysfunction. The crosstalk between autophagy and apoptosis is complex, and Hu et al. revealed that autophagy or autophagy-related proteins can lead to apoptosis or autophagic cell death under certain conditions [11].

AMP-activated protein kinase (AMPK), a key regulator of energy metabolism in the heart, is involved in the regulation of many cellular processes. As both anti-apoptotic and pro-apoptotic actions of AMPK have been reported, cardiomyocytes exposed to hyperglycaemia and oxidative stress under diabetic conditions can trigger both autophagy and apoptosis [8]. Despite of an increasing interest in the potential role of AMPK in the pathogenesis of diabetes and the possible use of AMPK-stimulating agents as treatment for this disease, this is the first study to demonstrate that exogenous H_2S leads to a significant increase in AMPK activity in the cardiac tissue of rats with increasing autophagosomes in type I diabetes. This finding supports the idea that increasing autophagy in cardiomyocytes through pharmacological activation of AMPK could be a novel strategy for the treatment of type I diabetes.

Hydrogen sulphide (H_2S) is the third endogenous gas to be identified as an important cell signalling molecule [12, 13]. H_2S is produced naturally in mammalian tissues and exhibits various biological and physiological effects [14-17], such as modulated metabolic state [18], mitochondrial function, cellular redox status, and cell apoptosis [19].

High glucose induces formation of reactive oxygen species (ROS), whereas H_2S represents a remarkable capacity to scavenge ROS. As a gasotransmitter with exclusive biologic effects, H_2S can be endogenously generated by cystathionine-β-synthetase (CBS) and cystathionine-γ-lyase (CSE) in mammalian tissues [13, 20, 21].

In the diabetic cardiovascular system, little information is available for the relationship between H_2S and autophagy. Therefore, we utilized *in vivo* and *in vitro* studies to identify the involvement of autophagy with H_2S treatment during cardiac dysfunction. We also investigated the potential mechanism(s) of action in H_2S -facilitated autophagy with a focus on the AMPK–mTOR pathway.

Materials and Methods

Animals and ethics statement

One hundred and twenty male Wistar rats were purchased by Harbin Medical University (8 weeks of age weighing 200-250 g). The rats were fed with a normal rat diet and had free access to water under conditions of standard temperature (20–22˚C) and humidity (50-60%) in standard lighting (alternating 12 h light/dark cycle). After one week of acclimatization, the rats were fasted overnight before the experiments. The animal protocol was reviewed and adheres to the Declaration of Helsinki and International Ethical Guidelines for Biomedical Research. This study protocol was approved by the Animal Ethics Committee of Harbin Medical University.

Determination of blood glucose

Random, morning blood glucose, non-fasting, concentration obtained from tail veins was determined at 4- to 8-week intervals in all groups by Roche AccuChek ® Inform (Roche Diagnostics, Indianapolis, IN).

Reagents

Sodium hydrosulfide (NaHS), Streptozotocin (STZ; Sigma Chemical), GYY4137 (morpholin-4-ium-4-methoxyphenyl morpholino phosphinodithioate), bafilomycin A1 (02911643), DL-proparglycine (PPG) were purchased from Sigma Chemical (St. Louis, MO). Hoechst 33342, Propidium iodide (PI) and 2, 7-dichlorofluorescein diacetate (DCFH-DA) were obtained from Beyotime (Shanghai, China). N-acetylcysteine (NAC), siRNA AMPK were purchased from Cell Signalling Technology (Beverly, MA). Lipofectamine 2000 and JC-1 were both obtained from Invitrogen (Carlsbad, CA). CSE, Beclin-1, AMP-activated protein kinase (AMPK), p-AMPK (Thr172), p62 , LC3 , mammalian target of rapamycin (mTOR), p-mTOR p70-S6 Kinase，phospho-p70 S6K，4EBP, phospho-4EBP antibodies are provided by Cell Signalling Technology (Beverly, MA, USA). Cytochrome c, pro-caspase-3/9 and cleavage-caspase 3/9 antibodies were provided by Proteintech Group (Chicago, IL). DMEM-F12 medium and fetal bovine serums (FBS) were supplied by Hyclone (Logan, UT).

Establishment of STZ-induced type I diabetes animal model

Streptozotocin (STZ; Sigma Chemical) dissolved in citrate buffer (pH 4.5) and diluted in 0.3 ml of normal saline (0.9% NaCl injection USP, Baxter) was administered intraperitoneally at a dose of 50 mg/kg body weight. The rats were randomly divided into three groups as follows: control group (n=40; neither injected with STZ nor treated with NaHS), diabetic group (Dia group; n=40; injected with STZ), diabetes + NaHS group (Dia+NaHS group; n=40; injected with STZ and administered with NaHS). Successful generation of a type I diabetic model occurred when a blood glucose level of 16.7 mM was obtained 72 hrs after STZ injection [22], and blood glucose levels ranged from 5 to 10 mM in the control group injected with saline only [23]. Rats with blood glucose levels <6 mM were non-diabetic and used as controls.

Daily administration in the NaHS treatment groups

In the NaHS treatment group, rats were given the intraperitoneal injection of NaHS (100 μM) with dosages based on a previous study [24] and our preliminary experiments [25]. Briefly, age-matched diabetic rats and control rats were sacrificed after treatment for 4 and 8 weeks. For every blood sample, the serum was obtained after centrifugation, and the serum was stored at -80°C. Each left ventricular was subjected to 3 tests as follows: western blotting for autophagic and apoptotic-related proteins; haematoxylin and eosin staining; and transmission electron microscopy (TEM).

Transmission electron microscopy

The mixed cells and left ventricular myocardial tissues were collected and fixed in 2.5% glutaraldehyde under transmission electron microscopy. After dehydrated through an ascending ethanol series and embedded in epoxy resin, ultrathin sections were cut and stained with uranyl acetate and lead citrate. All ultrastructural analyses were performed in a blinded and nonbiased manner from photomicrographs captured using the Philips CM120 electron microscope.

Measurement of H_2S content

After 4 and 8 weeks, the plasma and myocardial contents of H_2S were measured by methylene blue as described by Chunyu [26] with modifications [27]. Briefly, tissues were homogenized in ice-cold 100 mM potassium phosphate buffer (pH 7.4). The assay mixture (500 μl) contained tissue homogenate (450 μl), l-cysteine (10 mM; 20 μl), pyridoxal 5′-phosphate (2 mM; 20 μl), and saline (30 μl). Incubation was carried out in tightly sealed eppendorf vials. After incubation (37 °C, 20min), 1% zinc acetate (250 μl) was injected to trap evolved H_2S. This was followed followed by 10% trichloroacetic acid (250 μl) to precipitate protein and stop the reaction. Thereafter, N,N-dimethyl-p-phenylenediamine sulfate (20 mM;133 μl) in 7.2 M HCl was added followed by $FeCl_3$ (30 mM; 133 μl) in 1.2 M HCl and absorbance (670 nm) of aliquots of the resulting solution (300 μl) was determined after 10 mins using a 96-well microplate reader (Costar, USA). The same procedure was applied to measure the plasma H_2S level. All chemicals and reagents were obtained from Sigma (USA).

Western blot analysis

Protein homogenates were prepared from left ventricular tissue, and the protein concentration of the cell lysates was then determined using a BCA protein assay reagent kit (Beyotime，China). Equal amounts of protein (50 μg) were loaded on 10 % SDS-PAGE gels, transferred onto nitrocellulose membranes and

blocked with 5 % non-fat milk. The membranes were incubated with primary antibodies overnight at 4 °C. The membranes were then incubated with horseradish peroxidase-conjugated anti-rabbit or anti-mouse secondary antibodies at room temperature for one hour. In this study, β-actin and VDAC were served as loading control for the cytosolic and mitochondrial fraction, respectively.

Separation of Mitochondrial Protein from Cardiac Tissues

Isolation of mitochondrial protein from left ventricular tissue was performed according to a mitochondria isolation kit (Beyotime Inc., Shanghai, China). The cardiac tissues (n=4-5, per group) were washed twice with ice-cold PBS, resuspended in lysis buffer, and then homogenized by an homogenizer in ice water. After removing the nuclei and cell debris by centrifugation at 1, 000 g for 10 min at 4°C, the supernatants were further centrifuged at 10, 000 g for 20 min at 4°C. Th protein concentration was determined using the Bicinchoninic acid (BCA) assay kit (Beyotime Inc., Shanghai, China).The resulting mitochondrial pellets were resuspended in lysis buffer,which was stored on ice and used for experiments within 4 h.

Mitochondrial respiration measurements

A Clark oxygen electrode was used for examining the oxygen consumption of mitochondria [28]. Mitochondria were incubated in respiration buffer (100 mM KCl, 25 mM sucrose, 5 mM KH_2PO_4, 1 mM $MgCl_2$, 1 mM EGTA, 10 mM HEPES, 10 mM glutamate, and 2.5 mM malate) [29], and state 3 of respiration (consumption of oxygen in the presence of substrate and ADP) was initiated with ADP (75 nmol/mg protein). States 3 and 4 (consumption of oxygen after ADP phosphorylation) respiration, respiratory control ratio (RCR = state 3/state 4), and ADP/O index (a marker of the mitochondrial ability to couple oxygen consumption to ADP phosphorylation during state 3 respiration) were determined according to Chance and Williams (1956) [30].

Cell culture and Treatment

H9C2 cells have been shown to retain several electrical and hormonal characteristics similar with adults' cardiomyocytes. In current study, we used H9C2 cells to establish high glucose model. H9C2 cells (Chinese Academy of Medical Sciences, Shanghai, China) were cultured in Dulbecco's Modified Eagle Media supplemented with 10% FBS and 100 μg/mL penicillin&streptomycin (Beyotime , China) at 37°C under an atmosphere of 5% CO_2 and 95% O_2. H9C2 Cells were cultured to 70–80% confluence and treated with either high glucose (40 mM) or H_2S (dissolved in phosphate buffered saline) in combination.For inhibitor experiments, H9C2 cells were pre-incubated with a selective autophagy inhibitor, 3-MA (10 μM), or an AMPK inhibitor, compound C (2.5 μM), PPG (0.3 mM) and then treated without or with H_2S together with high glucose. The stimulant concentration of high glucose (40 mM) for H9C2 cells was determined from our pilot studies.

Analysis of cell viability

Cell viability was determined using a short-term microculture tetrazolium (MTT) assay. Cells were seeded into 96-well plates at a density of 2.5 x 10^4 cells/well and incubated in 100 μl of culture media then exposed to different concentrations of glucose for varying time periods. The viability of H9C2 cells was determined by adding MTT to the cell cultures to reach a final concentration of 1 mg/ml. After the MTT-containing DMEM was removed, the remaining dark crystals formed were dissolved in 75 μl HCl/isopropyl alcohol solution. Optical densities at 570 nm were measured by a plate reader with an appropriate filter.

Assessment of apoptosis

Morphological changes of apoptosis including cellular morphological change,

chromatin condensation chromosomal condensation of H9C2 cells, were observed by Hoechst 33342 staining followed by fluorescent microscope. In brief, after different treatments, H9C2 cells were washed after three-time washes with ice cold PBS, cells were resuspended in 1 ml of PBS solution with Hoechst 33342 /PI and the cells were visualized under a fluorescent microscope.

Measurement of intracellular reactive oxygen species (ROS)

After different treatments, cells were incubated with 10 μM Probes 2′, 7′- dichlorofluorescin diacetate (DCFH-DA; Beyotime, Shanghai, China) in a 37°C humidified incubator for 30 mins and washed twice with phosphate-buffered saline, pH 7.4 [31]. The slides were washed three times with PBS and DCF fluorescence

was measured over the entire field of vision by using a fluorescence microscope connected to an imaging system (BX50-FLA, Olympus, Tokyo, Japan). Mean fluorescence intensity (MFI) from three random fields was analyzed by Image pro plus， and MFI was used to represent the amount of ROS. The experiment was carried out three times.

JC-1 Mitochondrial Staining

We assessed the mitochondrial membrane potential using JC-1 as described below. Mitochondrial membrane potential (MMP, Ψm) is the main indicator of mitochondrial metabolism [32]. MMP was assessed using a fluorescent dye, JC-1, a cell-permeable cationic dye that preferentially enters the mitochondria based on the highly negative MMP. Depolarization of MMP results in the loss of JC-1 from the mitochondria and a decrease in intracellular fluorescence. The cells were seeded on a slide with DMEM. After the indicated treatments, the slides were washed three times in PBS. Cells were stained with 5 μM JC-1 dye by incubating at 37 °C for 15 min. The dye changed reversibly from red to green as the mitochondrial membrane became depolarized. Fluorescence was measured using a fluorescence microscope and the MFI of JC-1 from 5 random fields was analysed using ImagePro Plus software.

Monodansylcadaverine (MDC) assay for visualization of autophagic vacuoles

Autophagosomes in the cells were detected by MDC staining using the method as previously described [33]. Briefly, the cells were incubated with 0.05 mM MDC (Sigma) in Hanks' buffered salt solution at 37 °C for 10 mins. After being washed three times with 0.1 M PBS, MDC-labelled autophagosomes were examined by a fluorescence microscope and counted in x200 fields (five sequential fields were counted and averaged per coverslip) for three coverslips in each experiment as a percentage of total cell number.

Detection of H_2S in H9C2 cells using a 7-Azido-4-Methylcoumarin H_2S probe

Intracellular free H_2S levels were determined using 7-Azido-4-methylcoumarin (C-7Az). This probe is used both to monitor enzymatic production of H_2S *in vitro* [34] and to visualize H_2S in cells [35]. After the indicated treatments, H9C2 cells were washed with PBS and incubated with 50 μM AzMc combined with a surfactant at 37 °C for 20 mins in the dark. The MFI of 4 random fields was measured over the entire field of vision and analysed by Image pro plus software.

AMPK short interfering RNA transfection

AMPK siRNA (a pool of 3 target-specific19–25 nucleotide siRNAs designed to knockdown the gene expression of mitofusin-2 in rats) and scrambled control were purchased from Cell Signalling Technology, Inc. (Beverly, MA). Transient transfection was initially standardized to improve knockdown efficiency. Subsequently, all the transient transfections were performed with 150 nM AMPK siRNAs using Lipofectamine 2000 (Invitrogen) according to the manufacturer's protocol. After 6 hours, the transfection mixtures were replaced with regular medium. After 48 hours' transfection, cells were incubated with medium containing 5 or 40 mM glucose for 24 hours. Cells were processed for assessment of mitochondrial networks and protein expression.

Statistical analysis

All values were given as the means ± the standard error of the mean (S.E.M.) for at least three replicates. Statistical data was analyzed with Newman t –test or ANOVA as appropriate using Graph Pad Prism 5 for Windows platform (Graph Pad Software, San Diego, CA). $P<0.05$ was considered statistically significant.

Results

Establishment of the STZ-induced type I diabetic cardiomyopathy model

A well-established type I diabetes mellitus model of STZ injection was used in this study. As expected, levels of blood glucose significantly increased in long-term STZ-induced diabetic rats. Meanwhile, an obvious decrease in body weight was found when compared with control rats (Table 1), confirming their diabetic state. Heart weight and blood glucose levels in 8 weeks diabetic rats were similar to those of 4 weeks diabetic rats, and these

Table 1. Characterization of the experimental animal models. Blood glucose levels (mg/dl) obtained via tail vein puncture, body weight (g), heart weight (g), Food intake(g/day) and water intake(g/day) during the study period at 4- to 8-week intervals. Experimental groups were compared with their corresponding values after 4 and 8 weeks. Values are given as the means ± S.E.M. n=8. * P<0.05 vs. control group; # P<0.05 vs. Dia group, respectively (n=6)

	Control	Dia 4wks	Dia 8wks
Body weight (g)	223.3 ± 8.69	183.3 ± 14.72*	187 ± 14.05*
Heart weight (g)	0.94 ± 0.09	0.74 ± 0.17*	0.78 ± 0.09*
Glucose (mg/dl)	4.3 ± 0.70	24.3 ± 4.81*	21 ± 2.09*
Food intake(g/day)	13.2 ± 1.5	39.4 ± 2.3*	46.8 ± 2.5*
Water intake(ml/day)	27 ± 3.0	183 ± 4.9*	228 ± 5.6*

Table 2. Echocardiographic assessment of cardiac function. Effect of NaHS on the cardiac left ventricle function. Dia, diabetes; LVEDD is the LV end-diastolic dimension and LVESD is the end-systolic LV dimension. * P<0.05 vs. control group; # P<0.05 vs. Dia group, respectively (n=3)

	Control	Dia 4wks	Dia+NaHS 4 wks	Dia 8wks	Dia+NaHS 8 wks
LVEF	75.7 ± 4.1	69.5 ± 4.8*	65.9 ± 3.7*	71.0 ± 4.2*	72.8 ± 2.2*
LVFS	40.1 ± 2.1	37.7 ± 3.1*	31.1± 2.7*	38.7 ± 3.51*	38.56± 2.38*
LVEDD	7.43 ± 0.27	8.4 ± 0.47*	8.7 ± 0.33*	8.1 ± 0.56	8.3 ± 0.33
LVESD	3.77 ± 0.28	4.31 ± 0.99*	4.29 ±0.46*	4.13 ± 0.15*	4.07 ± 0.23
E/A ratio	1.52 ±0.17	1.42 ±0 .11*	1.40 ± 0.15*	1.45 ±0.24	1.48 ±0.71

levels were higher than those of the control group (Table 1). Echocardiography was used to assess cardiac structure and function (Table 2). LVEDD was significantly increased in the 4 wks and 8wks Dia groups compared with control group. However, LVESD was significantly increased in the 4 wks Dia group but decreased in the 4 wks Dia+ NaHS group (P< 0.05). Left ventricular Ejection Fraction (LVEF) and Left Ventricular Fractional Shortening (LVFS) were both decreased in the Dia and Dia+NaHS group. Administration of NaHS modestly increased the LVEF in the 8 wks Dia+NaHS group compared to the 8 wks Dia group (P>0.05). Furthermore, the E/A ratio was decreased in the 4 wks Dia groups compared to the control, and the indexes increased in the 4 wks Dia+NaHS group compared to the diabetic groups (P< 0.05).

Hydrogen sulphide level and expression of CSE in rat cardiac tissue

Hydrogen sulphide content was determined by methylene blue and sulphide electrode methods. Our results showed that H_2S contents in plasma and myocardial tissue were significantly lower in the Dia group than in the control group. However, in the Dia+ NaHS group, H_2S levels were markedly higher than those in the Dia group (Fig. 1A-D).

The expression of CSE proteins in cardiac tissues decreased in the 4 and 8 wks Dia groups compared to the control group (P< 0.05). The expression of myocardial CSE increased significantly in the Dia+NaHS groups compared to the diabetes groups (P<0.05) after 4 and 8 weeks of exogenous H_2S treatment (Fig. 1E).

Exogenous H_2S supplementation increases autophagic vacuoles in diabetic rats

Transmission electron microscopy revealed that there were some autophagic vacuoles (two-layer membrane structures that wrap around partially degraded cargo) in the sections from the experimental groups. In contrast, there was no evident abnormality in the control

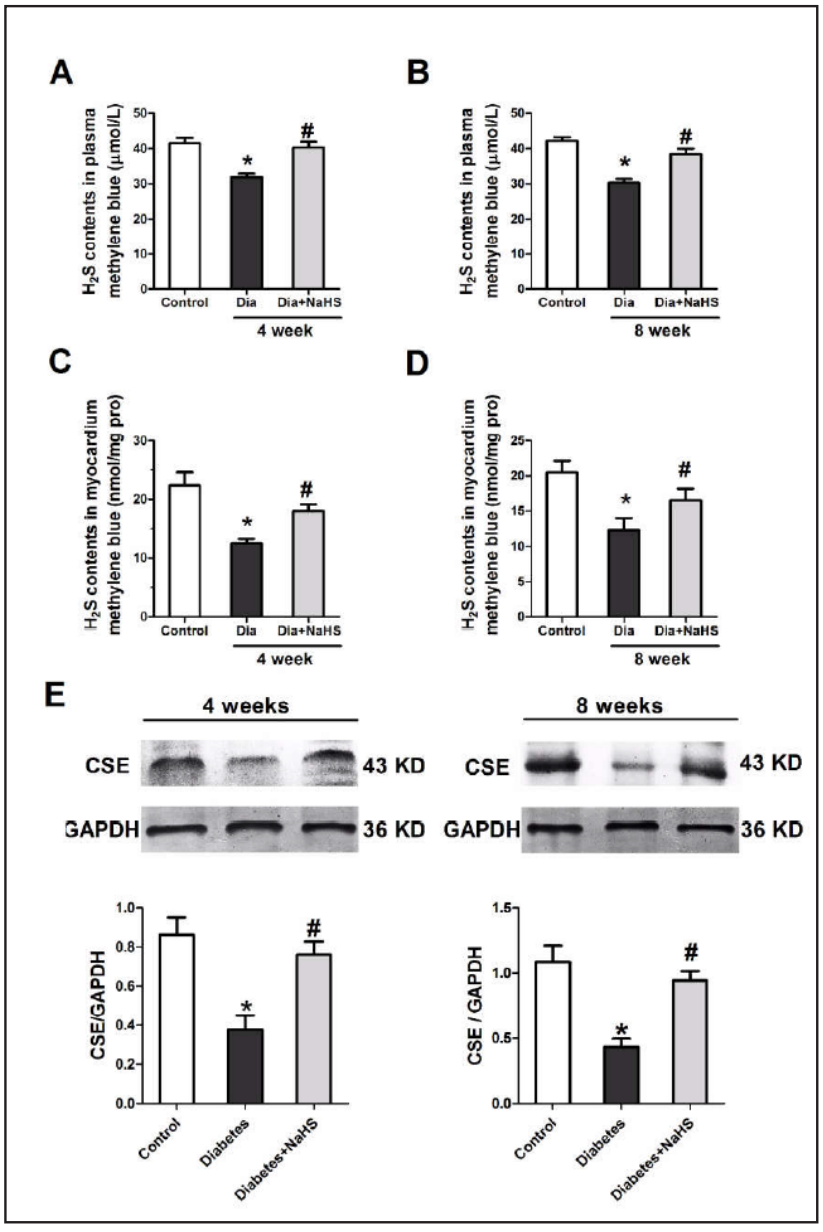

Fig. 1. Hydrogen sulphide level and the expressions of CSE in rats cardiac tissue. (A-D). Alteration of plasma and myocardium H_2S level during the study period at 4- to 8-week intervals. Dia and Dia+NaHS groups were compared with the corresponding values of the control group. Experimental groups were compared with their corresponding values after 4 and 8 weeks. Values are given as the means ± S.E.M. n=5. * P<0.05 vs. control group; #P<0.05 vs. diabetes group (E). The expression of CSE proteins in cardiac tissues in 4- and 8-week diabetic groups compared with control (P< 0.05). Dia, diabetes.* P<0.05 vs. control group; # P<0.05 vs. Dia group, respectively (n=3).

group. The percentage of autophagic vacuoles per cytoplasm area was significantly increased in the Dia+NaHS groups compared to the diabetic group (Fig. 2A). The expression of Beclin-1 was significantly increased *in vivo* in the Dia+NaHS groups compared to the Dia group (Fig. 2B). Moreover, the expression of p-AMPK/AMPK was decreased in the diabetic groups, whereas administration of NaHS significantly increased the expression of p-AMPK/AMPK (Fig. 2C).

Exogenous H_2S ameliorates respiratory chain impairment induced by hyperglycaemia.

In a first approach to investigate the impact of H_2S on mitochondrial bioenergetic function, mitochondrial respiration and oxidative phosphorylation were evaluated in freshly isolated cardiac mitochondria energized with succinate, a complex II substrate. Mitochondrial coupling and oxidative phosphorylation were measured and indicated by the RCR and ADP/O indexes, respectively. ΔΨm results in the conversion of ADP to ATP via ATP synthase, which is essential for oxidative phosphorylation occurrence. Mitochondrial respiratory chain pumps H^+ out of the mitochondrial matrix across the inner mitochondrial

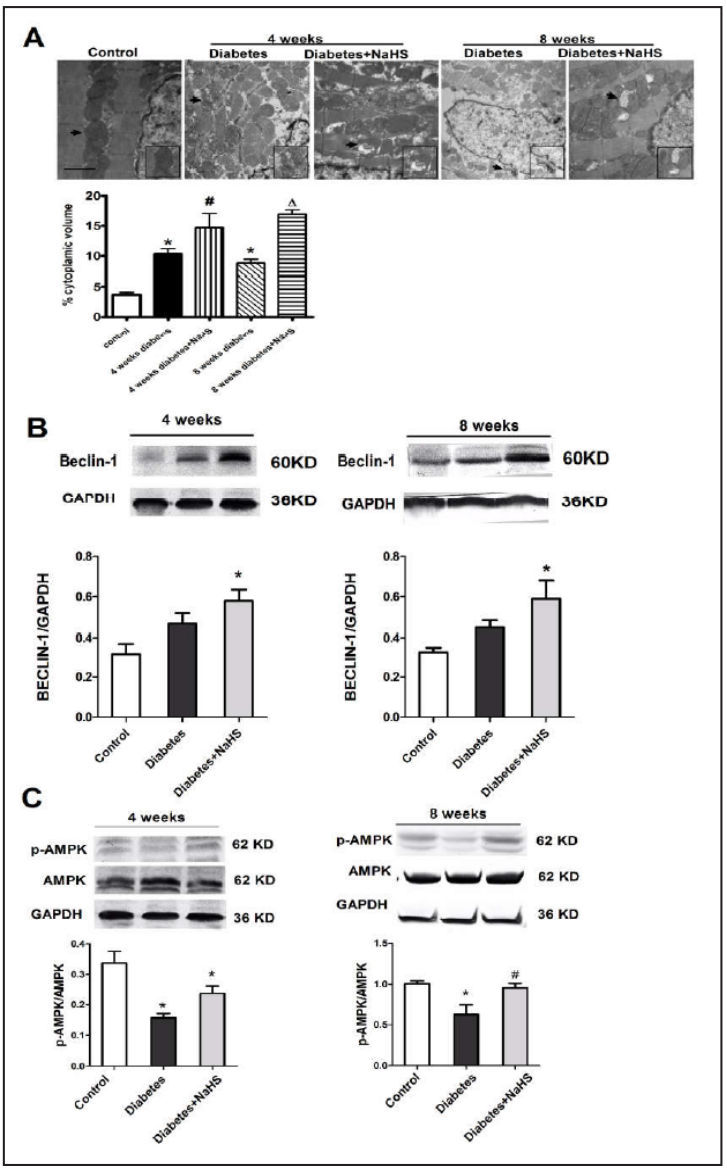

Fig. 2. Accumulation of autophagic vacuoles positively correlates with the level of H_2S. (A) Representative TEM photographs of cardiac tissues harvested from the Dia and Dia+NaHS groups. The percentage of autophagic vacuoles per cytoplasm area was totalled, bar: 2 μm. (B) Cardiac tissues were obtained from control, Dia, and Dia+NaHS groups after 4 or 8 weeks. Western blots of Beclin-1 and p-AMPK/AMPK were examined. The upper trace of each group show representative blots of the respective protein, and the lower panels show the bar graphs summarizing the immunoblot data. Densitometry results are expressed as a fold increase (*P<0.05 vs. control group; #P<0.05 vs. Dia group).

membrane. Our results showed that state 3 respiration was decreased significantly in cardiac mitochondria in long-term hyperglycaemic rats and that state 4 respiration was increased compared to Dia+NaHS groups (Fig. 3A&B). The RCR and ADP/O index decreased in the diabetes groups, which indicated that the respiratory chain was impaired (Fig. 3C&D).

GYY4137 increases cell viability and prevents MMP collapse in the presence of high glucose group

To explore the effect of HG on cell viability, H9C2 cells were treated with normal (5.5 mM), 25 mM and 40 mM glucose for 24 and 48 hrs. Cell viability decreased by 21% and 35% in the 40 mM HG treatment groups after 24 and 48 hrs compared to the LG groups (Fig. 4A). Therefore, we selected two time points, namely 24 and 48 hrs, for autophagic observation (Fig. 4D) by MDC. Based on the data in Fig. 4A, 40 mM HG treatment for 48 hrs caused significant cell injury (measured by cell viability). We selected 40 mM HG treatment for 48 hrs as our model group for further research as these conditions were suitable to mimic the hyperglycaemia in DC.

It has been reported that GYY4137 releases H_2S slowly in aqueous solution *in vitro* [36]. Release of H_2S from GYY4137 in aqueous solution is pH-dependent with considerably

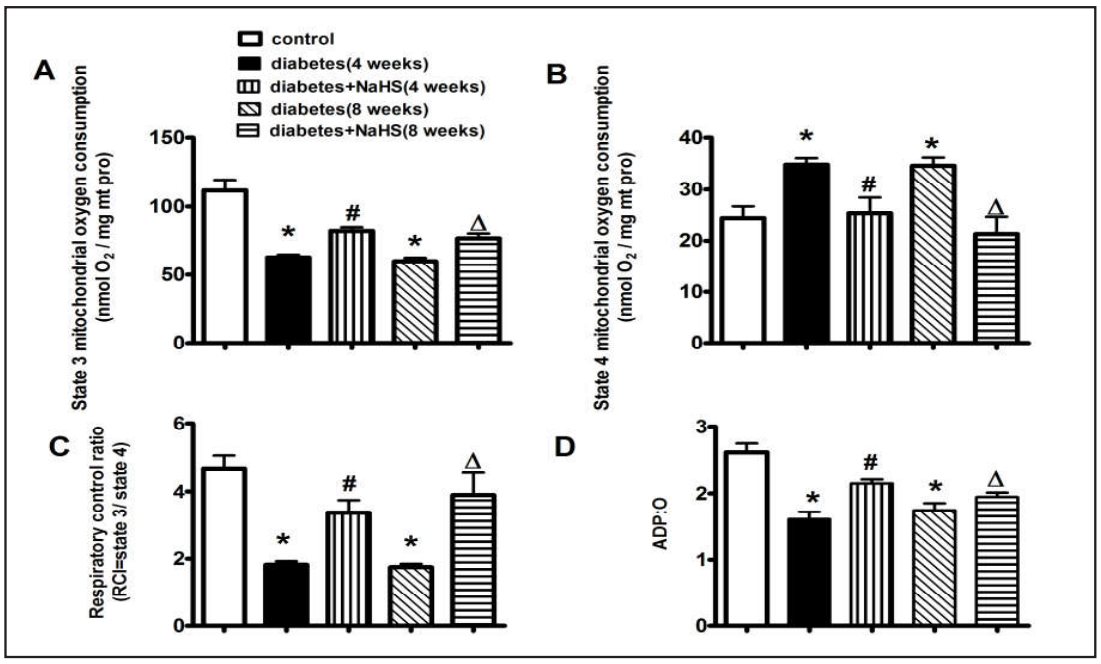

Fig. 3. Effect of long-term hyperglycaemia and NaHS treatment in cardiac mitochondria respiratory chain parameters: States 3 (A) and 4 (B) of respiration, RCI(C) and ADP/O index (D). * P<0.05 vs. control; # P<0.05 vs. 4 weeks diabetes group; ΔP<0.05 vs. 8 weeks diabetes group. Data are the mean ± SEM of 5–6 animals from each condition studied.

greater release at pH 3.0 than at neutral or alkaline pH [37]. GYY4137 is more expensive but causes long-lasting relaxation of cells *in vitro* compared to NaHS. Thus, in this study, we used GYY4137 to further examine the role of H_2S in high glucose-treated H9C2 cells, and we used NaHS to examine the role of H_2S in rats. When H9C2 cells were incubated with 50, 100, and 200 μM GYY4137 for 48 hrs, cell viability (Fig. 4B) and MMP collapse were improved in the HG-treated group in a concentration-dependent manner (Fig. 4E&F). However, treatment with 100 μM GYY4137 alone had no such effects. As shown in Fig. 4E, mitochondria were considerably damaged after 40 mM HG treatment for 48 hrs, and MMP collapse was prevented by different concentrations of GYY4137 treatment. Our results suggested that 100 μM GYY4137 protects mitochondrial function and significantly increases cell viability of cells treated with high glucose. As shown in Fig. 4C, GYY4137 increased autophagosomes compared to the HG group. GYY4137 treatment after 48 hrs further increased autophagy under HG, indicating that H_2S at least in part increased autophagy production under HG. Therefore, we selected 100 μM GYY4137 for further research. Autophagic vacuoles detected by MDC were increased after treatment with GYY4137 100 μM for 48 hrs (Fig. 4D). Thus, 48 hrs was used as the endpoint for observation *in vitro*.

Detection of H_2S level in H9C2 cells using fluorescence microscopy

As shown in Fig. 5 A, the mean fluorescence intensity was significantly increased in the high glucose-cultured group but was decreased after 48 h treatment with GYY4137. In addition, the exogenous supply of GYY4137 can be converted into H_2S through enzymatic H_2S biosynthesis in cells. Our results revealed that the H_2S level in cells treated by HG was significantly decreased, and these alterations were attenuated after treatment with GYY4137 (Fig. 5B).

H_2S inhibits high glucose-induced cell apoptosis in H9C2 cells

ROS releases in high glucose states are related to various cardiac diseases. Reducing oxidative stress leads to significant reduction of heart pathology in degenerative diseases

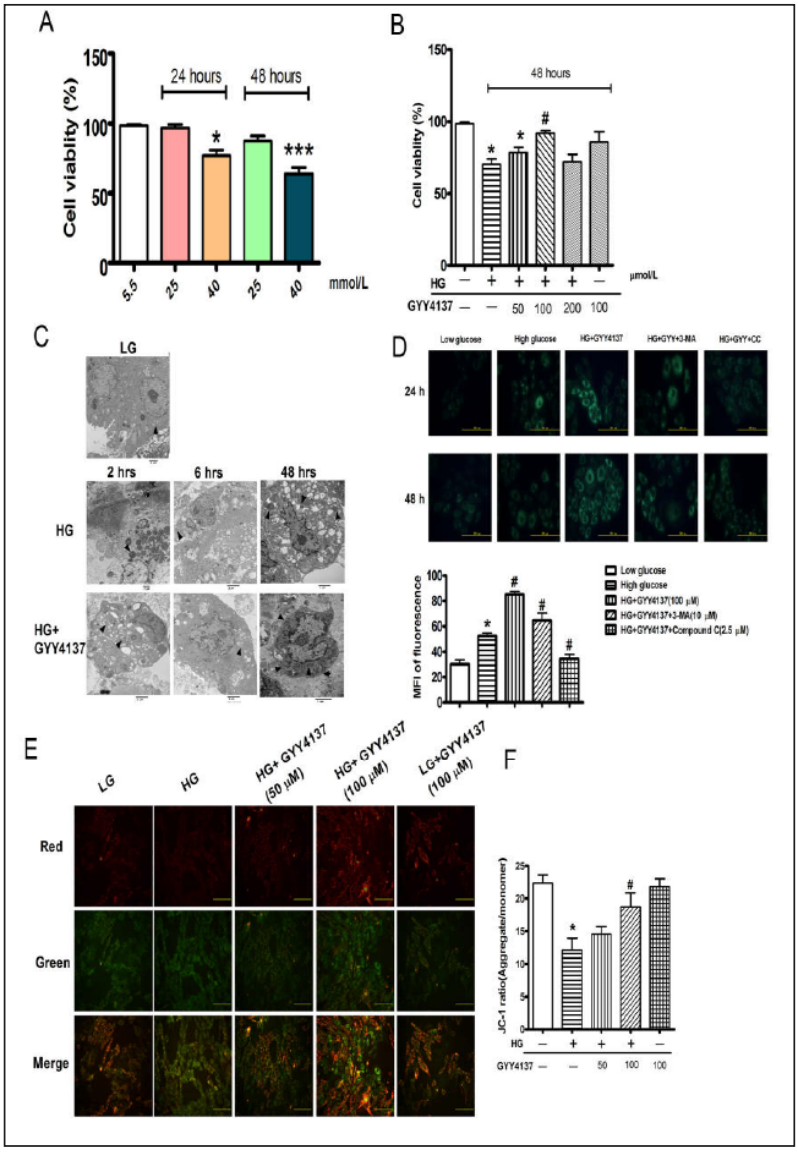

Fig. 4. GYY4137 treatment attenuates HG-induced cell viability decreases and MMP collapse in a concentration-dependent manner (A) Cell viability measurement in control (5.5 mM glucose) and high glucose group at various concentrations during 24 and 48 hours. (B) H9C2 cells were incubated in control medium (5.5 mM glucose) or HG medium (40 mM glucose) with or without the indicated GYY4137 concentrations (μM) for 48 h. Cell viability was quantified using the MTT assay kit. (C) Ultrastructural changes in H9C2 cells cultured during 48 hrs. TEM revealed that cells in the 5.5 mM glucose (LG) group exhibited clear structures of H9C2 cells but that the nuclear contour was deformed and mitochondria were swollen in the 40 mM glucose group (HG). In the HG+GYY4137 group, mitochondria were slightly swollen, and autophagosomes were present. Black arrows represent autophagosomes. (D) Representative micrographs of MDC fluorescence in H9C2 cells. LG, 5.5 mM glucose; HG, 40 mM glucose; HG+GYY4137, H9C2 cells were pre-treated with 100 μM GYY4137 for 30 min; HG+GYY4137+3-MA, cells were treated with 10 μM 3-MA; HG+GYY4137+AICAR, cells were treated with 2.5 μM AICAR. All groups were treated for 48 hrs, and quantitative analysis of the mean fluorescence intensity was obtained in the indicated groups. Data are the means ± S.E.M. (n=3). * P<0.05 compared with LG, # P<0.05 compared with HG. (E-F) JC-1 measured the mitochondrial membrane potential (ΔΨm). The effect of GYY4137 treatment on mitochondrial membrane potential in H9C2 cells treated with HG. JC-1 spontaneously forms J-aggregates and exhibits red fluorescence (590 nm) under a high membrane potential. The JC-1 monomeric form shows green fluorescence (528 nm) under a low potential. The red fluorescence to green fluorescence ratio was measured. (* p< 0.05 vs. control group. # p< 0.05 vs. HG group).

[12]. The levels intracellular ROS in H9C2 cells cultured with high glucose for 24 hrs and 48 hrs were determined (Fig. 5C). As expected, exogenous H_2S treatment significantly reduced high glucose-induced intracellular ROS levels (P<0.05). H9C2 cells cultured in high glucose were also treated with the ROS scavenger NAC (100 μM). Intracellular ROS levels increased

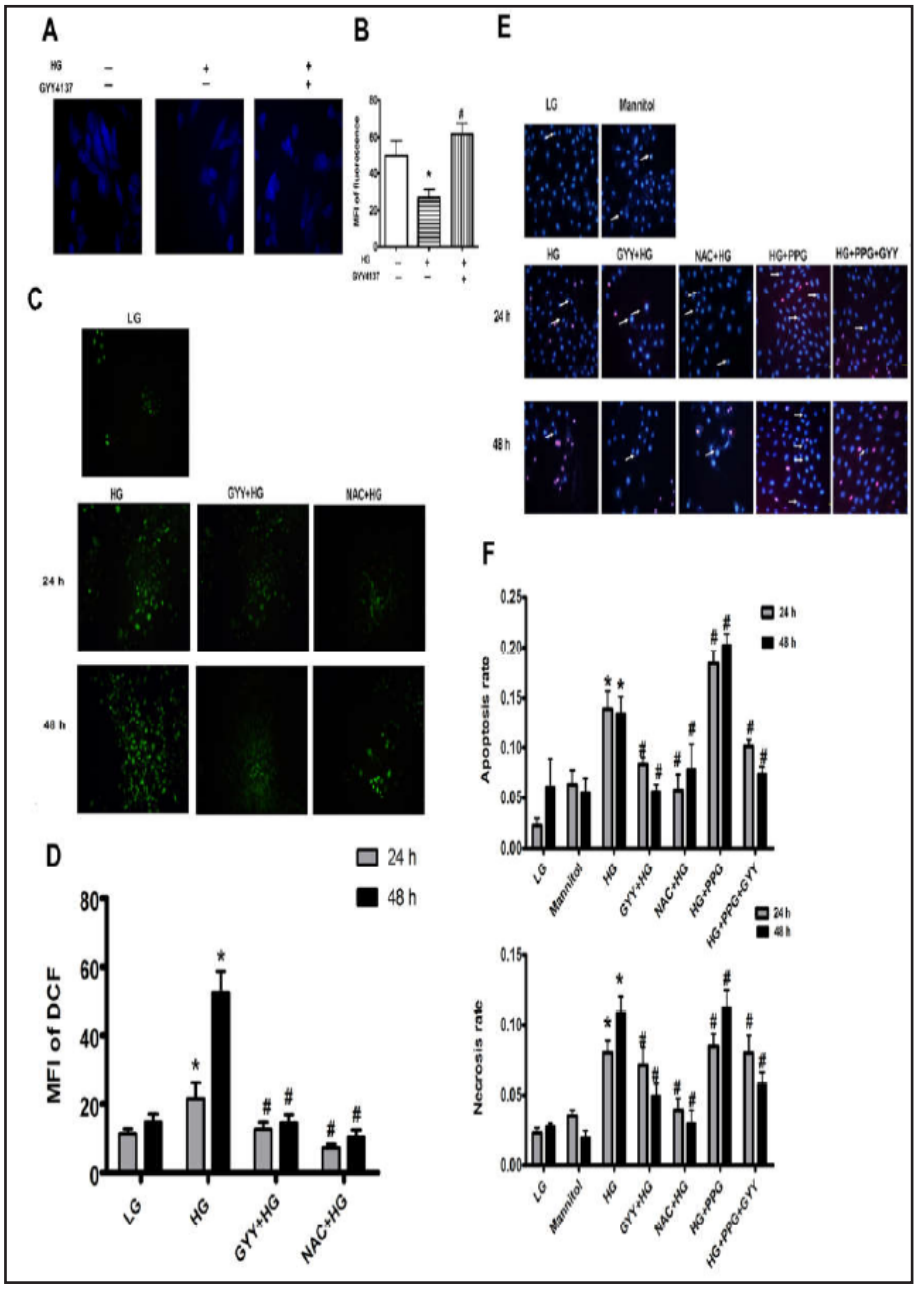

Fig. 5. GYY4137 treatment attenuates HG-induced ROS generation and apoptosis in H9C2 cells. (A) H9C2 cells were treated with 40 mM glucose and 100 μM GYY4137 for 48 hours, and the H_2S levels were measured (* p< 0.05 vs. control group. # p< 0.05 vs. HG group). (B) ROS levels were measured by DCFH (green fluorescence). The mean fluorescence intensity was measured. Data were summarized from at least three different experiments (* P<0.05 vs. LG group; # P<0.05 vs. HG group). (C) H9C2 cell apoptosis was assessed using Hoechst/PI staining for the following groups: Mannitol group; LG, 5.5 mM glucose; HG, 25 mM glucose; HG+GYY4137, H9C2 cells were pre-treated with 100 μM GYY4137 for 30 min; and HG+NAC, cells were treated with 100 μM NAC. All groups were treated for 24 hrs or 48 hrs. Summary data showing Hoechst-positive cells (%total counted cells) and PI-positive cells from 10 visual fields of 5 different areas. Values are means ± S.E.M * P<0.05 vs. the LG group. # P<0.05 vs. the HG group (n=3). Original magnification ×200.

significantly 48 hrs after exposure to 40 mM DMEM. The NAC treatment group also reduced hyperglycaemia-induced ROS accumulation (Fig. 5D).

Moreover, our results showed the protective effect of H_2S on high glucose-induced cell death in H9C2 cells. H9C2 cells were exposed to high glucose and then treated with H_2S for the indicated time period. Cell viability was assayed by a MTT assay. As shown in Fig. 4B, treatment of H9C2 cells with H_2S markedly reduced high glucose-induced cell injury. H_2S also

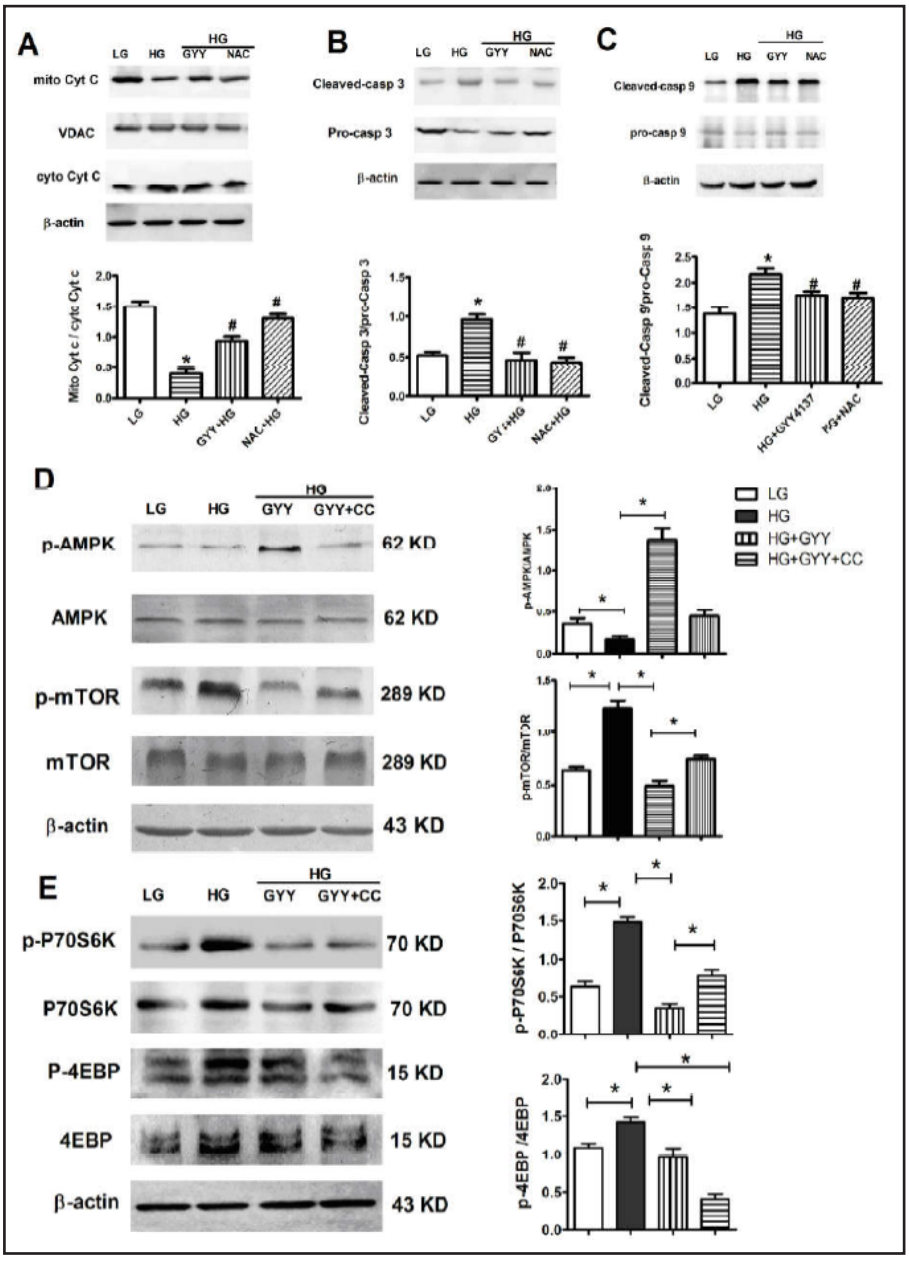

Fig. 6. GYY4137 treatment attenuates HG-induced ROS generation and apoptosis in H9C2 cells. (A-C) High glucose induces apoptosis via caspase-3 and -9 activation and increased mitochondrial cytochrome C (cyt C) release into cytosol. H9C2 cells were treated with 5.5 mM glucose (lane 1), 40 mM glucose (lane 2), 100 μM GYY4137 (lane 3) and 100 μM NAC (lane 4) for 48 hrs. β-Actin served as the loading control. Data are representative of three separate experiments (* P<0.05 vs. LG group; # P<0.05 vs. HG group). (D) Western blots analysis of p-AMPK/AMPK and p-mTOR/mTOR proteins in H9C2 cells. LG, Low glucose; HG, high glucose; HG+GYY, H9C2 cells were pre-treated with 100 μM GYY4137 for 30 min; HG+GYY+CC, cells were treated with 2.5 μM compound C. Densitometry results are expressed as a fold increase. Data are the means ± S.E.M. (n=3) (Significance at *P＜0.05).(E) The p-P70S6K and p-4EBP levels were examined by Western blotting. LG, low glucose; HG, high glucose; HG+GYY, high glucose+GYY4137; HG+GYY+CC, high glucose+GYY4137+Compound C. Data are representative of at least three different experiments (Significance at *P＜0.05).

protected against high glucose-induced cellular apoptosis (Fig. 5E). DL-proparglycine (PPG), an irreversible competitive CSE inhibitor, was used to further investigate the role of H_2S in inhibiting apoptosis and inducing autophagy. For the PPG group, cells were pre-treated with PPG (0.3 mM) for 60 mins before high glucose induction was administered. The induction of apoptosis is a major event in the response of H9C2 cells to hyperglycaemic stress. Thus, we investigated the role of apoptosis in PPG-treated cells by Hoechst/PI staining. Necrotic cell

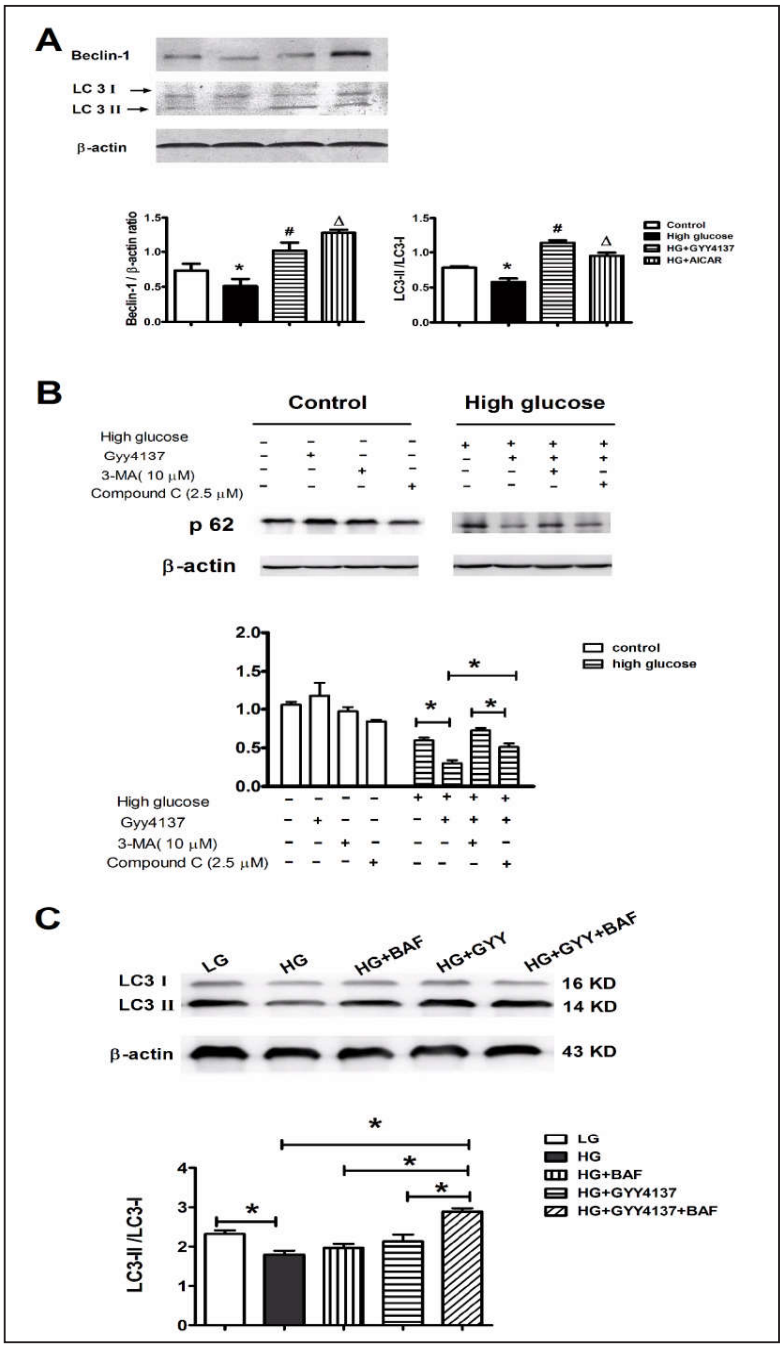

Fig. 7. Protective autophagic effect of GYY4137 on high glucose induced H9C2 cell injury. (A) H9C2 cells were treated with 5.5 mM glucose (lane 1), 40 mM glucose (lane 2), 100 μM GYY4137 (lane 3) and HG+20 μM AICAR(lane 4) for 48 hrs. β-Actin served as the loading control. Beclin-1 and LC II/I antibodies represent protein levels in HG, GYY4137 and AICAR treatment groups in H9C2 cells cultured. Data are representative of three separate experiments. * P<0.05 vs. the LG group; #P<0.05 vs. the HG group; ΔP<0.05 vs. the HG+GYY4137 group (n=4). (B) P62 expression in H9C2 cells in different treatment groups. The upper trace of each group shows a representative blot of p62 protein, and the lower panel shows the bar graph summarizing the immunoblot data. Densitometry results are expressed as a fold increase. Data are the means ± S.E.M. (n=3). * P<0.05 vs. control group; # P<0.05 vs. diabetes group. (C) The LC3 level was examined by Western blotting. Each value was standardized to actin. LG, low glucose; HG high glucose; HG+BAF, high glucose + bafilomycin A1; HG+GYY4137 + BAF, high glucose + GYY4137 + bafilomycin A1. Data were summarized from at least three different experiments (Significance at *P＜0.05).

death was as detected by propidium iodide (PI). Fig. 5E shows that the apoptotic cells increased in HG+PPG cells compared to GYY4137-treated cells after 24 or 48 hrs. However, GYY4137+PPG treatment did not significantly affect cell apoptosis compared to the PPG group (Fig. 5F). Viable cells displayed normal nuclear size and uniform fluorescence in the control group, whereas apoptotic cells showed condensed, fractured, or distorted nuclei in the high glucose group. White arrows indicate the fragmented and condensed nuclei by Hoechst staining. Our results showed that the H_2S-treated group showed low levels

of cytochrome C release from the mitochondria into the cytoplasm compared to the HG group (Fig. 4A). Our data showed that high glucose significantly induced pro-caspase 3 and pro-caspase 9 cleavages in H9C2 cells (Fig. 6B&C). Our data confirmed that high glucose activated caspase-3 and caspase-9 in H9C2 cells, and H_2S suppressed this activation. These results indicated that H_2S inhibits oxidative stress, which attenuates apoptosis induced by high glucose.

H_2S mediated activation of autophagy during high glucose-induced pathogenesis via the AMPK/mTOR pathway

AMPK, a major regulator of cellular energy homeostasis, is known to activate autophagy, and inhibition of mTOR is associated with autophagy induction [38]. We examined the phosphorylations levels of AMPK and mTOR to elucidate the molecular autophagy mechanism induced by H_2S during high glucose *in vitro*. The ratio of p-AMPK/AMPK was decreased after HG induction, while the ratio of p-mTOR/mTOR was significantly increased in high glucose group. To determine the involvement of mTOR signalling in H_2S-mediated activation of autophagy during high glucose-induced pathogenesis, Compound C (CC), an inhibitor of AMPK, was used to determine the involvement of mTOR signaling in H_2S-induced activation of autophagy during high glucose treatment (Fig. 6D).

Interestingly, the activity of the mTOR pathway was dramatically increased by high glucose, as indicated by decreased phosphorylation of P70S6K (a downstream substrate of mTOR Complex 1) and 4EBP (a downstream target of mTOR Complex 1), compared to low glucose. After treatment with GYY4137 or pre-treatment with CC, these indexes decreased compared to those in the high glucose treatment alone group (Fig. 6E). Therefore, mTOR signalling acted as a downstream effector of AMPK signalling in regulation of autophagy mediated by the administration of H_2S during high glucose treatment.

H_2S induces autophagy in H9C2 cells in an AMPK-dependent manner

Autophagy usually improves cell survival, and recent studies have reported that autophagy protects cells from apoptosis [39, 40]. LC3 is initially synthesized in its unprocessed form, and cardiac autophagy is suppressed as evidenced by a decrease in conversion of LC3-I to LC3-II [41]. LC3-II is localized in the autophagosome membrane and serves as a reliable protein marker of autophagy. LC3-II can be degraded in autolysosomes during autophagy [42]. Therefore, treatment with the autophagic inhibitor, 3-MA, or CC will enhance the level of LC3-II if H_2S increases autophagic flux. H9C2 cells were treated with GYY4137 (100 μM) and AICAR (AMPK activator, 20 μM) for 48 hrs. Cells showed an increase in the Beclin-1/β-actin ratio and LC3II/I ratio compared to cells treated with high glucose alone (Fig. 7A). In addition, a significantly decreased p62/β-actin ratio was observed after high glucose treatment. The p62/β-actin ratio indicated that GYY4137-induced autophagy was significantly decreased by 3-MA or CC pre-treatment. There was no significant autophagy after treatment with 3-MA or CC alone for 24 hrs compared to control cells (both $P > 0.05$). Our results indicated that H_2S induces autophagy in H9C2 cells in an AMPK-dependent manner (Fig. 7B).

To determine autophagic flux after exogenous H_2S addition, we cultured cells in the absence or presence of BAF (100 nM) DMEM with low glucose (5.5 mM) and high glucose (40 mM) for 48 hrs. BAF markedly increased LC3 II levels in cells treated with GYY4137, whereas BAF had only a small effect on LC3 II content when cells were exposed to high glucose, suggesting that H_2S-mediated induction of LC3 II levels was attributed mainly to increased AV formation rather than reduction of lysosome degradation (Fig. 7C).

AMPK knockdown leads to autophagy inhibition and cell dysfunction

To determine if AMPK is responsible for the autophagic induction by H_2S, H9C2 cells were transfected with AMPK siRNA. As shown in Fig. 8A, cells exhibited a profound decrease of AMPK. These results strongly suggested that AMPK activation is essential for a protective effect of H_2S in H9C2 cells under oxidative stress. In addition to H_2S, knockdown of AMPK

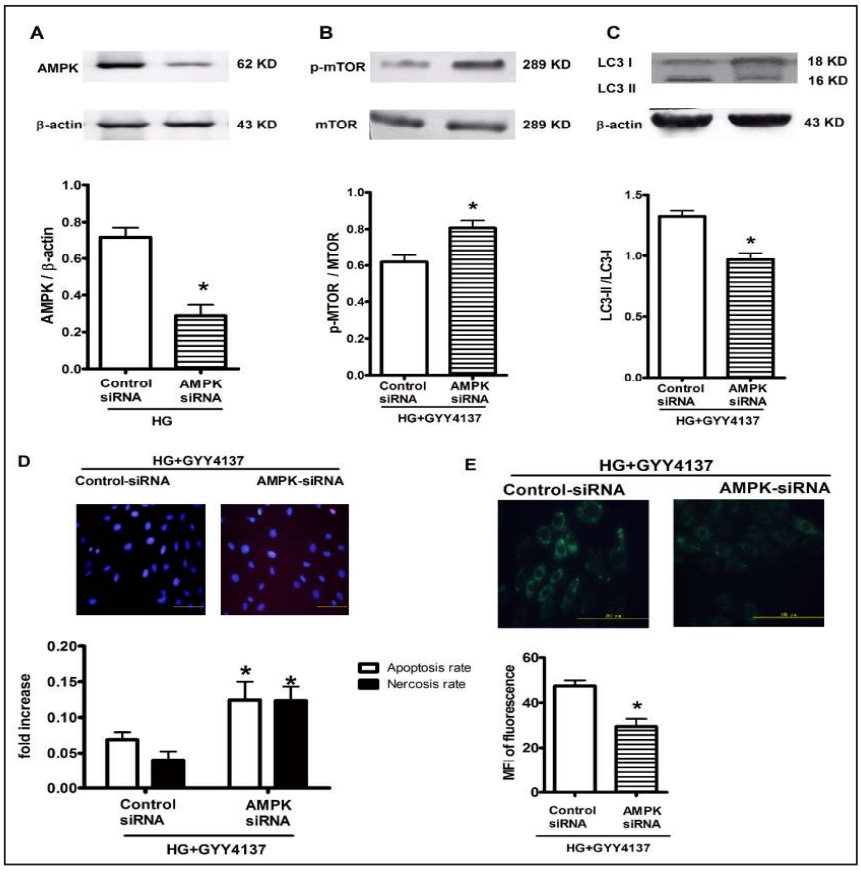

Fig. 8. Effects of AMPK siRNA on GYY4137-elicited cardioprotection. (A-C) H9C2 cells were transfected with AMPK siRNA and cultured under high glucose conditions. H9C2 cells were treated with HG+control-siRNA (lane1) and HG+150 nM AMPK siRNA (lane 2) for 48 hrs. (B) H9C2 cells were transfected with AMPK siRNA and cultured under high glucose+GYY4137. H9C2 cells were treated with control-siRNA (lane 1) and HG+150 nM AMPK siRNA (lane 2) for 48 hrs. (C) H9C2 cells were transfected with AMPK siRNA and cultured under high glucose+GYY4137. H9C2 cells were treated with HG+control-siRNA (lane 1) and HG+150 nM AMPK siRNA (lane 2) for 48 hrs. β-Actin served as the loading control. The upper trace of each group shows representative blots of the respective proteins, and the lower panels show the bar graphs summarizing the immunoblot data. Densitometry results are expressed as a fold increase. * P<0.05 vs. control siRNA group. (D) Cell apoptosis was assessed using Hoechst/PI staining for control-siRNA and150 nM AMPK siRNA groups under HG+GYY4137. The analysis of fold increase in H9C2 cells. (E) Cell autophagy was assessed using MDC staining for HG+control siRNA and HG+150 nM AMPKsiRNA groups. All groups were treated for 48 hrs. Summary data showing Hoechst-positive cells (% total counted cells) and PI-positive cells from 10 visual fields of 5 different areas. Values are means ± S.E.M * P< 0.05 vs. control siRNA group. (n=3). Original magnification×200.

increased the ratio of p-mTOR/mTOR, while the ratio of LC3-II/LC3-I was significantly reduced (Fig. 8B&C). These results demonstrated that H_2S-induced autophagy is linked to the AMPK pathway. Knockdown of AMPK in cells led to an augmentation of apoptosis (Fig. 8D), thereby suggests the involvement of AMPK-dependent autophagy in cardioprotection.

Discussion

Diabetic cardiomyopathy is a critical complication of diabetes [43]. A comprehensive understanding of mechanisms underlying the pathogenesis of diabetic cardiomyopathy is urgently needed. Our study presented three major findings. Firstly, NaHS administered after high glucose treatment elevated serum levels of H_2S and protected against hyperglycaemia injury. Secondly, cardioprotection conferred by the H_2S donor, NaHS and GYY4137, was dependent on AMPK activation *in vivo* and *in vitro*. Finally, H_2S suppressed high glucose

injury by activating autophagy via the AMPK/mTOR pathway, which is likely the mechanism underlying cardioprotection conferred by H_2S.

H_2S exerts a wide influence on the cardiovascular system [44, 45]. There is ample evidence that cardiovascular disease is related to decreased expression of CSE [46, 47]. Our previous studies have found that H_2S regulates the interactions and cause a switch among cell death pathways during hyperglycaemia [25, 32]. In the present study, we established a classic type I diabetic rat model to investigate the protective effects of H_2S against hyperglycaemia-induced cardiac dysfunction. GYY4137 is a well-known H_2S donor that has vasodilatory and antihypertensive activities [37]. We selected GYY4137 as our tool to explore the cardiovascular biology of H_2S *in vitro* as it reflected endogenous physiological release.

Our findings indicated that administration of NaHS increased H_2S contents in plasma and myocardial tissue in diabetic rats (Fig. 1A-D) and that H_2S could protect against left ventricular systolic dysfunction in the diabetic group according to echocardiographic data (Table 2).

Previous studies have shown that mitochondria are involved in the process of high glucose injury through enhancing the production of mitochondrial ROS and opening of the mPT pore [25]. The formation of ROS from cardiomyocytes is a key factor in the pathogenesis of diabetic complications [43, 48, 49]. In this study, we surprisingly found that high glucose decreased mitochondrial oxidative phosphorylation efficiency, induced mitochondrial swelling, promoted mitochondrial Cyt C release and promoted ROS generation (Fig. 5B&Fig. 6A). In contrast, the administration of exogenous H_2S to isolated mitochondria significantly improved mitochondrial state 3 respiration in a concentration-dependent manner (Fig. 3). These results strongly indicated that there may be a causal relationship between mitochondrial dysfunction and anomalous generation of ROS in high glucose injury. Elevated levels of mitochondrial ROS could damage the mitochondrial membrane and associate with increased mitochondrial membrane permeabilization. In response to high glucose, autophagosomes chelate ROS-generating mitochondria to protect cells, while 3-MA increases the production of ROS and advances apoptosis [50]. Cellular apoptosis associated with oxidative stress in multiple organs of diabetes mellitus has been documented [51, 52]. Autophagy inhibition in isolated cardiomyocytes has been shown to increase apoptosis and necrosis, while autophagy inhibition has also been shown to be protective in some studies [53, 54]_ENREF_50. Although H_2S has been demonstrated to inhibit apoptosis and necrosis, it remained unclear if autophagy is involved in H_2S-triggered protection [55]. In our study, we demonstrated that H_2S activated cytoprotective autophagy *in vivo* and *in vitro*. Autophagy was evaluated by the following methods: TEM and MDC fluorescence evaluation of autophagosomes provided a valid insight into what events were happening inside in the cell; and western blot analysis was used to interpret the molecular changes as indicated by LC3 induction and p62 degradation. Our results further supported that autophagy is a homeostatic mechanism for maintaining cardiac function by managing cellular injury.

To date, several cellular signalling pathways are speculated to turn on autophagy under high glucose [54]. AMP-activated protein kinase (AMPK) exerts its biological effects in cardiovascular functional regulation. Activation of AMPK inhibits diabetes-induced cardiomyocyte apoptosis and prevents cardiac dysfunction in diabetic animals after treatment with metformin [9], suggesting that further investigations are needed to explain the role of AMPK in the regulation of autophagy and apoptosis. Interestingly, our previous study demonstrated that H_2S inhibits induction of protein synthesis in the endothelial cells after high glucose treatment by activation of AMPK [56]. Indeed, activation of AMPK inhibits mTOR, the negative regulator of autophagy, and subsequently stimulates autophagy. Moreover, synergistic effects are observed when H_2S treatment is combined with an AMPK inhibitor. Our current study demonstrated that inhibition of AMPK phosphorylation and obverted phosphorylation of mTOR in response to high glucose injury (Fig.6 D&E).

Compound C and 3-MA were applied in the high glucose model to confirm the role of autophagy in the cardioprotection-induced by H_2S via the AMPK-mTOR pathway. These compounds potently reduced the cytoprotective effects of H_2S. Cardiac autophagy was

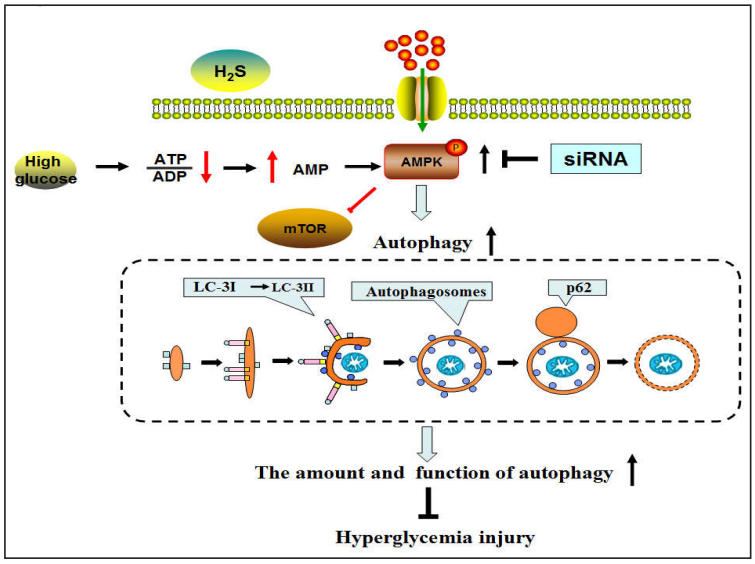

Fig. 9. The diagram of the proposed pathway which hydrogen sulfide exerts its inhibitory effect on autophagy in H9C2 cells. The diagram shows signal-transduction events associated with high glucose-induced injury. Hydrogen sulfide-induced autophagy elicited cytoprotective effects through activated-AMPK-mTOR pathway, and suggested a novel mechanism of H_2S-induced cytoprotection against high glucose injury.

suppressed as evidenced by a decrease in conversion of LC3-I to LC3-II [5]. The decreased LC3 conversion and expression of Beclin-1 after treatment with GYY4137 or AICAR in the present of high glucose was attributed to alterations in the formation of autophagosomes (Fig. 7A) .The upstream activity of autophagy processes was determined by the significant alterations of p62 (Fig. 7B). Our results agreed with previously published studies as they showed that compound C and 3-MA resulted in cardiac dysfunction by blocking autophagy activation [57].

Based on the aforementioned results, we postulated that the GYY4137-elicited cytoprotective effects against high glucose might be due to autophagy activation via the AMPK-mTOR pathway. Thus, we further investigated the role of AMPK in the protection of diabetic cardiomyopathy. Finally, AMPK siRNA increased mTOR phosphorylation and successfully inhibited autophagy, leading to increased apoptosis and cell injury (Fig. 8A-B). Thus, these results suggested that the AMPK-mTOR pathway participates in H_2S -induced autophagy regulation (Fig. 9). However, the role of autophagy is still controversial in cardiovascular diseases. Autophagy as a repair mechanism is activated with low intensity stress. With increasing stress levels, apoptosis begins to occur. Under extreme stress, ATP depletion results in necrosis and neither autophagy nor apoptosis can progress [58].

In conclusion, autophagy may be essential in H_2S-induced cardioprotection against high glucose injury. H_2S-activated AMPK-mTOR-dependent pathway may attribute to the regulatory mechanism for HG-induced autophagy. Therapeutic H_2S or autophagy activation may offer a promising new strategy in diabetic heart disease treatment. In addition, further studies are needed to examine the association between H_2S-induced autophagy and the AMPK-mTOR pathway in both type I and type II diabetes.

Acknowledgements

The project is supported by the grants from National Science Foundation of China (81370330, 81370421, and 81670344). Graduate innovation Foundation of Harbin Medical University (YJSCX2014-05HYD)

Disclosure Statement

No conflicts of interest, financial or otherwise, are declared by the author(s).

References

1 Joshi M, Kotha SR, Malireddy S, Selvaraju V, Satoskar AR, Palesty A, Maulik N: Conundrum of pathogenesis of diabetic cardiomyopathy: role of vascular endothelial dysfunction, reactive oxygen species, and mitochondria. Mol Cell Biochem 2014;386:233-249.
2 Mizushige K, Yao L, Noma T, Kiyomoto H, Yu Y, Hosomi N, Ohmori K, Matsuo H: Alteration in left ventricular diastolic filling and accumulation of myocardial collagen at insulin-resistant prediabetic stage of a type II diabetic rat model. Circulation 2000;101:899-907.
3 Avogaro A, Vigili de Kreutzenberg S, Negut C, Tiengo A, Scognamiglio R: Diabetic cardiomyopathy: a metabolic perspective. Am J Cardiol 2004;93:13A-16A.
4 Picano E: Diabetic cardiomyopathy. the importance of being earliest. J Am Coll Cardiol 2003;42:454-457.
5 Mizushima N, Yoshimori T, Levine B: Methods in mammalian autophagy research. Cell 2010;140:313-326.
6 Kroemer G, Marino G, Levine B: Autophagy and the integrated stress response. Mol Cell 2010;40:280-293.
7 Epstein PN, Overbeek PA, Means AR: Calmodulin-induced early-onset diabetes in transgenic mice. Cell 1989;58:1067-1073.
8 Ouyang C, You J, Xie Z: The interplay between autophagy and apoptosis in the diabetic heart. J Mol Cell Cardiol 2014;71:71-80.
9 He C, Zhu H, Li H, Zou MH, Xie Z: Dissociation of Bcl-2-Beclin1 complex by activated AMPK enhances cardiac autophagy and protects against cardiomyocyte apoptosis in diabetes. Diabetes 2013;62:1270-1281.
10 Xie Z, Lau K, Eby B, Lozano P, He C, Pennington B, Li H, Rathi S, Dong Y, Tian R, Kem D, Zou MH: Improvement of cardiac functions by chronic metformin treatment is associated with enhanced cardiac autophagy in diabetic OVE26 mice. Diabetes 2011;60:1770-1778.
11 Hu P, Zhou H, Lu M, Dou L, Bo G, Wu J, Huang S: Autophagy Plays a Protective Role in Advanced Glycation End Product-Induced Apoptosis in Cardiomyocytes. Cell Physiol Biochem 2015;37:697-706.
12 Calvert JW, Coetzee WA, Lefer DJ: Novel insights into hydrogen sulfide--mediated cytoprotection. Antioxid Redox Signal 2010;12:1203-1217.
13 Huang Z, Zhuang X, Xie C, Hu X, Dong X, Guo Y, Li S, Liao X: Exogenous Hydrogen Sulfide Attenuates High Glucose-Induced Cardiotoxicity by Inhibiting NLRP3 Inflammasome Activation by Suppressing TLR4/NF-kappaB Pathway in H9c2 Cells. Cell Physiol Biochem 2016;40:1578-1590.
14 Kamoun P: H2S, a new neuromodulator. Med Sci (Paris) 2004;20:697-700.
15 Wang R: Two's company, three's a crowd: can H2S be the third endogenous gaseous transmitter? FASEB J 2002;16:1792-1798.
16 Szabo C: Hydrogen sulphide and its therapeutic potential. Nat Rev Drug Discov 2007;6:917-935.
17 Yu Q, Lu Z, Tao L, Yang L, Guo Y, Yang Y, Sun X, Ding Q: ROS-Dependent Neuroprotective Effects of NaHS in Ischemia Brain Injury Involves the PARP/AIF Pathway. Cell Physiol Biochem 2015;36:1539-1551.
18 Blackstone E, Morrison M, Roth MB: H2S induces a suspended animation-like state in mice. Science 2005;308:518.
19 Kashfi K, Olson KR: Biology and therapeutic potential of hydrogen sulfide and hydrogen sulfide-releasing chimeras. Biochem Pharmacol 2013;85:689-703.
20 Tang C, Li X, Du J: Hydrogen sulfide as a new endogenous gaseous transmitter in the cardiovascular system. Curr Vasc Pharmacol 2006;4:17-22.
21 Wang R: The gasotransmitter role of hydrogen sulfide. Antioxid Redox Signal 2003;5:493-501.
22 Zheng D, Dong S, Li T, Yang F, Yu X, Wu J, Zhong X, Zhao Y, Wang L, Xu C, Lu F, Zhang W: Exogenous Hydrogen Sulfide Attenuates Cardiac Fibrosis Through Reactive Oxygen Species Signal Pathways in Experimental Diabetes Mellitus Models. Cell Physiol Biochem 2015;36:917-929.
23 Bhutada P, Mundhada Y, Bansod K, Bhutada C, Tawari S, Dixit P, Mundhada D: Ameliorative effect of quercetin on memory dysfunction in streptozotocin-induced diabetic rats. Neurobiol Learn Mem 2010;94:293-302.
24 Li F, Luo J, Wu Z, Xiao T, Zeng O, Li L, Li Y, Yang J: Hydrogen sulfide exhibits cardioprotective effects by decreasing endoplasmic reticulum stress in a diabetic cardiomyopathy rat model. Mol Med Rep 2016;14:865-873.
25 Yang F, Yu X, Li T, Wu J, Zhao Y, Liu J, Sun A, Dong S, Zhong X, Xu C, Lu F, Zhang W: Exogenous H_2S regulates endoplasmic reticulum-mitochondria cross-talk to inhibit apoptotic pathways in STZ-induced type I diabetes . Am J Physiol Endocrinol Metab 2017;312:e190-e203.

26 Chunyu Z, Junbao D, Dingfang B, Hui Y, Xiuying T, Chaoshu T: The regulatory effect of hydrogen sulfide on hypoxic pulmonary hypertension in rats. Biochem Biophys Res Commun 2003;302:810-816.
27 Mok YY, Atan MS, Yoke Ping C, Zhong Jing W, Bhatia M, Moochhala S, Moore PK: Role of hydrogen sulphide in haemorrhagic shock in the rat: protective effect of inhibitors of hydrogen sulphide biosynthesis. Br J Pharmacol 2004;143:881-889.
28 Poe M, Gutfreund H, Estabrook RW: Kinetic studies of temperature changes and oxygen uptake in a differential calorimeter: the heat of oxidation of NADH and succinate. Arch Biochem Biophys 1967;122:204-211.
29 Predmore BL, Kondo K, Bhushan S, Zlatopolsky MA, King AL, Aragon JP, Grinsfelder DB, Condit ME, Lefer DJ: The polysulfide diallyl trisulfide protects the ischemic myocardium by preservation of endogenous hydrogen sulfide and increasing nitric oxide bioavailability. Am J Physiol Heart Circ Physiol 2012;302:H2410-2418.
30 Chance B, Williams GR: The respiratory chain and oxidative phosphorylation. Adv Enzymol Relat Subj Biochem 1956;17:65-134.
31 Sun L, Zhao M, Yang Y, Xue RQ, Yu XJ, Liu JK, Zang WJ: Acetylcholine Attenuates Hypoxia/Reoxygenation Injury by Inducing Mitophagy Through PINK1/Parkin Signal Pathway in H9c2 Cells. J Cell Physiol 2016;231:1171-1181.
32 Zhong X, Wang L, Wang Y, Dong S, Leng X, Jia J, Zhao Y, Li H, Zhang X, Xu C, Yang G, Wu L, Wang R, Lu F, Zhang W: Exogenous hydrogen sulfide attenuates diabetic myocardial injury through cardiac mitochondrial protection. Mol Cell Biochem 2012;371:187-198.
33 Sicklick JK, Li YX, Melhem A, Schmelzer E, Zdanowicz M, Huang J, Caballero M, Fair JH, Ludlow JW, McClelland RE, Reid LM, Diehl AM: Hedgehog signaling maintains resident hepatic progenitors throughout life. Am J Physiol Gastrointest Liver Physiol 2006;290:G859-870.
34 Thorson MK, Majtan T, Kraus JP, Barrios AM: Identification of cystathionine beta-synthase inhibitors using a hydrogen sulfide selective probe. Angew Chem Int Ed Engl 2013;52:4641-4644.
35 Chen B, Li W, Lv C, Zhao M, Jin H, Du J, Zhang L, Tang X: Fluorescent probe for highly selective and sensitive detection of hydrogen sulfide in living cells and cardiac tissues. Analyst 2013;138:946-951.
36 Wei WB, Hu X, Zhuang XD, Liao LZ, Li WD: GYY4137, a novel hydrogen sulfide-releasing molecule, likely protects against high glucose-induced cytotoxicity by activation of the AMPK/mTOR signal pathway in H9c2 cells. Mol Cell Biochem 2014;389:249-256.
37 Li L, Salto-Tellez M, Tan CH, Whiteman M, Moore PK: Free Radic Biol Med 2009;47:103-113.
38 Xie Z, He C, Zou MH: AMP-activated protein kinase modulates cardiac autophagy in diabetic cardiomyopathy. Autophagy 2011;7:1254-1255.
39 Jin Y, Wang H, Cui X, Xu Z: Role of autophagy in myocardial reperfusion injury. Front Biosci (Elite Ed) 2010;2:1147-1153.
40 Towers CG, Thorburn A: Therapeutic Targeting of Autophagy. EBioMedicine 2016;14:15-23.
41 Gottlieb RA, Mentzer RM: Autophagy during cardiac stress: joys and frustrations of autophagy. Annu Rev Physiol 2010;72:45-59.
42 Mizushima N, Yoshimori T: How to interpret LC3 immunoblotting. Autophagy 2007;3:542-545.
43 van Melle JP, Bot M, de Jonge P, de Boer RA, van Veldhuisen DJ, Whooley MA: Diabetes, glycemic control, and new-onset heart failure in patients with stable coronary artery disease: data from the heart and soul study. Diabetes Care 2010;33:2084-2089.
44 Liu Y, Liao S, Quan H, Lin Y, Li J, Yang Q: Involvement of microRNA-135a-5p in the Protective Effects of Hydrogen Sulfide Against Parkinson's Disease. Cell Physiol Biochem 2016;40:18-26.
45 Wei X, Zhang B, Zhang Y, Li H, Cheng L, Zhao X, Yin J, Wang G: Hydrogen Sulfide Inhalation Improves Neurological Outcome via NF-kappaB-Mediated Inflammatory Pathway in a Rat Model of Cardiac Arrest and Resuscitation. Cell Physiol Biochem 2015;36:1527-1538.
46 Yang G, Wu L, Jiang B, Yang W, Qi J, Cao K, Meng Q, Mustafa AK, Mu W, Zhang S, Snyder SH, Wang R: H2S as a physiologic vasorelaxant: hypertension in mice with deletion of cystathionine gamma-lyase. Science 2008;322:587-590.
47 Zhao W, Zhang J, Lu Y, Wang R: The vasorelaxant effect of H(2)S as a novel endogenous gaseous K(ATP) channel opener. EMBO J 2001;20:6008-6016.
48 Poornima IG, Parikh P, Shannon RP: Diabetic cardiomyopathy: the search for a unifying hypothesis. Circ Res 2006;98:596-605.

49 Akhileshwar V, Patel SP, Katyare SS: Diabetic cardiomyopathy and reactive oxygen species (ROS) related parameters in male and female rats: A comparative study. Indian J Clin Biochem 2007;22:84-90.
50 Ravikumar B, Sarkar S, Davies JE, Futter M, Garcia-Arencibia M, Green-Thompson ZW, Jimenez-Sanchez M, Korolchuk VI, Lichtenberg M, Luo S, Massey DC, Menzies FM, Moreau K, Narayanan U, Renna M, Siddiqi FH, Underwood BR, Winslow AR, Rubinsztein DC: Regulation of mammalian autophagy in physiology and pathophysiology. Physiol Rev 2010;90:1383-1435.
51 Cai L, Chen S, Evans T, Deng DX, Mukherjee K, Chakrabarti S: Apoptotic germ-cell death and testicular damage in experimental diabetes: prevention by endothelin antagonism. Urol Res 2000;28:342-347.
52 Gustafsson AB, Gottlieb RA: Recycle or die: the role of autophagy in cardioprotection. J Mol Cell Cardiol 2008;44:654-661.
53 Xiao J, Zhu X, Kang B, Xu J, Wu L, Hong J, Zhang Y, Ni X, Wang Z: Hydrogen Sulfide Attenuates Myocardial Hypoxia-Reoxygenation Injury by Inhibiting Autophagy via mTOR Activation. Cell Physiol Biochem 2015;37:2444-2453.
54 Kobayashi S, Xu X, Chen K, Liang Q: Suppression of autophagy is protective in high glucose-induced cardiomyocyte injury. Autophagy 2012;8:577-592.
55 Zhang HX, Liu SJ, Tang XL, Duan GL, Ni X, Zhu XY, Liu YJ, Wang CN: H2S Attenuates LPS-Induced Acute Lung Injury by Reducing Oxidative/Nitrative Stress and Inflammation. Cell Physiol Biochem 2016;40:1603-1612.
56 Liu J, Wu J, Sun A, Sun Y, Yu X, Liu N, Dong S, Yang F, Zhang L, Zhong X, Xu C, Lu F, Zhang W: Hydrogen sulfide decreases high glucose/palmitate-induced autophagy in endothelial cells by the Nrf2-ROS-AMPK signaling pathway. Cell Biosci 2016;6:33.
57 Xie H, Xu Q, Jia J, Ao G, Sun Y, Hu L, Alkayed NJ, Wang C, Cheng J: Hydrogen sulfide protects against myocardial ischemia and reperfusion injury by activating AMP-activated protein kinase to restore autophagic flux. Biochem Biophys Res Commun 2015;458:632-638.
58 Nishida K, Yamaguchi O, Otsu K: Crosstalk between autophagy and apoptosis in heart disease. Circ Res 2008;103:343-351.